

Full-folding optical potential for preequilibrium nucleon scattering at low energies

M. Avrigeanu¹, A.N. Antonov², H. Lenske³, and I. řte  cu ¹

¹*Institute for Physics and Nuclear Engineering, P.O. Box MG-6, 76900 Bucharest, Romania*

²*Institute of Nuclear Research and Nuclear Energy, 1784 Sofia, Bulgaria*

³*Institut f  r Theoretische Physik, Universit  t Giessen, D-35392 Giessen, Germany*

Abstract

The real part of the optical potential for the nucleon-nucleus scattering at lower energies ($E_i < 100$ MeV) has been calculated including nucleonic and mesonic form factors by a double folding approach. Realistic density- and energy-dependent effective NN -interactions *DDM3Y*, *BDM3Y* and *HLM3Y* based on the Reid and Paris potentials are used in this respect. The effects of the nucleon density distribution and the average relative momentum on the folded potential have been analysed. A good agreement with the phenomenological potential of Lagrange-Lejeune, as well as with the parametrization of Jeukenne-Lejeune-Mahaux for both neutron and proton double-folded potentials is obtained. The results indicate that the strongly simplified model interactions used in preequilibrium reaction theory neglect important dynamical details of such processes.

PACS number(s): 13.75.Cs, 21.30.Fe, 24.10.Ht, 25.40.Ep, 25.40.Fq

The nucleon-nucleus optical model potential (OMP) is an important tool for understanding and interpreting the mechanism of the interaction between a nucleon and a nuclear system. The explicit forms of the t -matrices and nuclear matter g -matrices have been used through the folding procedures to obtain more realistic OMP for practical use in the nuclear reaction calculations [1]. Brieva and Rook [2] used the local density approximation (LDA) in order to apply to finite nuclei the nucleon-nucleon (NN) g -matrix effective interaction appropriate for a pair of nucleons interacting in infinite nuclear matter. Jeukenne, Lejeune and Mahaux (JLM) [3] recommended a simpler parametrized form of the isoscalar real component obtained from Brueckner-Hartree-Fock nuclear matter calculations, to be used for practical nuclear reaction calculations. Actually, the use of the free nucleon-nucleon t -matrix as a complex effective interaction has already been applied successfully to nucleon scattering at higher energies ($E_i > 100$ MeV), e.g. [4] and references therein.

Microscopic descriptions have become a standard approach for the description of reactions leading to discrete final states and giant resonance, respectively [5]. However, a different situation is encountered for more complex nuclear reactions involving multistep processes. In this paper, we consider the inclusion of a microscopic OMP into the description of preequilibrium emission processes. Hitherto, the complexity of such reactions has been considered to inhibit the use of microscopic methods. It is common practice to use strongly simplified models, for example the simplest 1 fm range Yukawa interaction has been chosen to describe the effective NN -interaction leading to particle-hole excitations in the frame of the Feshbach-Kerman-Koonin (FKK) model [6], its strength V_0 being the only free parameter adjusted to reproduce the experimental data. The large discrepancies still present at low incident energies ($E_i < 50$ MeV) in the systematics of the phenomenological V_0 values prove the necessity to consider a more realistic NN -interaction [7] which should be chosen consistently with the corresponding real part of the optical model potential. One may consider in this respect the density- and energy-dependent effective DDM3Y, BDM3Y and HLM3Y interactions based on the g -matrix elements of the Reid and Paris NN -potentials [8–10], which seem to be most successful for the nucleon-nucleus scattering within the low-density nuclear matter [8].

The present work concentrates on a comparison of folding OMPs from different interactions and density models. The intention is to derive a global model which describes reliably elastic scattering over a large range of incident energies and target masses. Once such a model is available, it can be applied on safer theoretical grounds to the various reaction channels of preequilibrium reactions. Obviously, the OMP in these channels cannot be determined directly by experimental means. A microscopic model will reduce the still persisting uncertainties. Moreover, the consistency between the interaction used in elastic scattering and the non-elastic processes is guaranteed.

Usually, effective NN interactions are parametrized in terms of meson exchange-type propagators. e.g. of Yukawa shape. Folding calculations for OMPs and transition potentials involve an averaging over the intrinsic momentum distribution of the target nucleons. Hence, a region of off-shell momenta is covered. Under such conditions the use of “on-shell” meson exchange propagators might lead to spurious effects because contributions from large off-shell momenta are overestimated. These effects are well-known from calculations of the free NN t matrix [13] and in Brueckner theory, e.g. [14,15]. In order to avoid these uncertainties one has to introduce vertex and nucleon form factors which regularize the large momentum

region. Their effect is to exclude contributions from small distances where the composite structure of mesons and nucleons would become visible.

For a OBE-type interaction the momentum space vertex cut-offs correspond to remove in coordinate space the singularities of Yukawa functions at the origin. The same effect is obtained by folding an r-space form factor to a Yukawa function. In our calculations we follow this prescription and use a double folding procedure with effective NN interactions and a form factor describing the intrinsic structure of the nucleon. We expect to take into account typical features of realistic NN potentials (e.g. [11–13]) of which the regularized Reid93 potential [12] includes explicitly a dipole form factor.

The main aim of this work is to study the effects of both nuclear and nucleon density distributions. Equally important is a reliable treatment of the non-local exchange contributions from anti-symmetrization. In order to avoid the complications of a non-local optical potential we use the local momentum approximation. Different prescriptions of the related quantities like the kinetic-energy density $\tau(r)$ and various approximations of the average relative momentum $k_{av}(r)$ [16,17], on the corresponding double-folding real OMP at lower incident energies ($E_i < 100$ MeV) are investigated in detail.

The general expressions for the direct and exchange double-folding (DF) real parts of the optical potential in terms of the nuclear densities $\rho_1(\mathbf{r}_1)$ and $\rho_2(\mathbf{r}_2)$ of the projectile and the target nucleus, respectively, and the effective NN -interaction $v(\mathbf{s}=\mathbf{R} + \mathbf{r}_2 - \mathbf{r}_1)$ are by assuming proportional proton and neutron densities [1,8],

$$U_{0(1)}^D(E, \mathbf{R}) = \delta_{0(1)} \delta_{0(2)} \int d\mathbf{r}_1 \int d\mathbf{r}_2 \rho_1(\mathbf{r}_1) \rho_2(\mathbf{r}_2) v_{00(01)}^D(\rho, E, \mathbf{s}), \quad (1a)$$

$$U_{0(1)}^{EX}(E, \mathbf{R}) = \delta_{0(1)} \delta_{0(2)} \int d\mathbf{r}_1 \int d\mathbf{r}_2 \rho_1(\mathbf{r}_1, \mathbf{r}_1 + \mathbf{s}) \rho_2(\mathbf{r}_2, \mathbf{r}_2 - \mathbf{s}) v_{00(01)}^{EX}(\rho, E, \mathbf{s}) \exp\left[\frac{i\mathbf{k}(\mathbf{R})\mathbf{s}}{M}\right], \quad (1b)$$

where $\delta_0=1$, $\delta_1=(N_1 - Z_1)/A_1$, $\delta_2=(N_2 - Z_2)/A_2$, $M=A_1 A_2 / (A_1 + A_2)$, $\mathbf{k}(\mathbf{R})$ is the incident relative momentum, and ρ_1 and ρ_2 in Eq. (1b) are the density matrices for the projectile and the target nucleus, respectively. If the projectile is a nucleon, in the point-like approximation, i.e. for $\rho(r)=\delta(\mathbf{r})$, these expressions are reduced to the single-folded (SF) form. In the frame of the LDA the SF procedure leads to the nuclear matter approximation (NM) [8].

In this work we have evaluated Eqs. (1) in momentum space [1,8,9] by means of the detailed procedure developed by Khoa *et al.* [9], and the following approximations. The effective NN -interaction has been obtained by using the isoscalar and isovector components of the direct v_{00}^D , v_{01}^D and exchange parts v_{00}^{EX} , v_{01}^{EX} of the M3Y interaction based on the results of the g -matrix calculations using either Reid or Paris NN -potential [8]. The energy- and density-dependent M3Y effective NN -interaction has been taken in the form

$$v_{00(01)}^{D(EX)}(\rho, E, r) = F(\rho) g(E) v_{00(01)}^{D(EX)}(r). \quad (2)$$

Three forms of the effective NN -interaction density dependence, namely DDM3Y1 and BDM3Y1 [9]

$$F(\rho) = \begin{cases} C[1 + \alpha \exp(-\beta\rho)], & \text{for DDM3Y1,} \\ C(1 - \alpha\rho), & \text{for BDM3Y1,} \end{cases} \quad (3a)$$

and the third one HLM3Y [10] with different density dependence for the isoscalar and isovector components

$$F(\rho) = \begin{cases} f_0(\rho) = s_0[1 + a_1^0(\rho/\rho_0)^{1/3} + a_2^0(\rho/\rho_0)^{2/3} + a_3^0(\rho/\rho_0)^1] \\ f_\tau(\rho) = s_\tau[1 + a_1^\tau(\rho/\rho_0)^{1/3}] \end{cases} \quad (3b)$$

where involved in the present work. The energy-dependent factor is taken to be a linear function of the incident energy per nucleon E of the form $g(E) = 1 - \gamma E$. The coefficient γ has the values 0.002 for the M3Y-Reid interaction, and 0.003 for the M3Y-Paris interaction.

The frozen-density approximation [1,8,9] has been adopted for the overlap density which enters the explicit form of the density-dependent factor $F(\rho)$, being taken as the sum of the densities of the two colliding nuclei at the midpoint of the intranucleonic separation. A widely used approximation for the calculation of the knock-on exchange term of the folded potential is that proposed by Campi and Bouyssy [16], which preserves the first term of the expansion given by Negele-Vautherin [17] for the realistic density-matrix expression

$$\rho(\mathbf{R}, \mathbf{R} + \mathbf{s}) = \rho(\mathbf{R} + \frac{\mathbf{s}}{2}) \hat{j}_1 \left(k_{av}(\mathbf{R} + \frac{\mathbf{s}}{2}) s \right), \quad (4)$$

where $\hat{j}_1(x) = 3(\sin x - x \cos x)/x^3$, and k_{av} defines the average relative momentum [16]

$$k_{av}(r) = \left[\frac{5}{3\rho(r)} \left(\tau(r) - \frac{1}{4} \nabla^2 \rho(r) \right) \right]^{\frac{1}{2}}. \quad (5)$$

The last quantity is a function of the density distribution $\rho(r)$, and the approximation used for the kinetic-energy density $\tau(r)$ for each participant in the interaction.

The Fermi-type nucleon density distribution corresponding to the parameters ρ_0 , $R_{1/2}$, and a given by either the Skyrme-Hartree-Fock systematics [20] or Negele parametrization [21] are compared in Figs. 1(a) and (b). The Fermi distribution for the target nucleus density, obtained by using the Negele parametrization [21] is shown in Fig. 1(c).

Different forms of the kinetic-energy density $\tau(r)$ have been adopted for the light projectiles and for the target nuclei. Thus, the modified Thomas-Fermi (MTF) approximation [18] has been considered for light projectiles

$$\tau(\rho) = \alpha \rho(r)^{\frac{5}{3}} + \beta \frac{|(\nabla \rho)|^2}{\rho}. \quad (6)$$

The values of the parameters α and β depend on the number of the constituent nucleons of the projectiles. Following the analysis of Krivine and Treiner [18], we used for the nucleon as a projectile $\alpha = 0$ and $\beta = 1/4$. For heavier nuclei and also within the MTF frame we have $\alpha = 3(3\pi^2)^{2/3}/5$. Consequently, the following expression have been obtained for $k_{av}(r)$ in the case of light projectiles (here nucleons)

$$k_{av}^{MTF}(r) = \left[\frac{5|\nabla \rho(r)|^2}{12\rho^2(r)} - \frac{5\nabla^2 \rho(r)}{12\rho(r)} \right]^{\frac{1}{2}}, \quad (7a)$$

while for heavier nuclei we have

$$k_{av}^{MTF}(r) = \left[k_F(r)^2 + \frac{5|\nabla\rho(r)|^2}{12\rho^2(r)} - \frac{5\nabla^2\rho(r)}{12\rho(r)} \right]^{\frac{1}{2}}, \quad (7b)$$

where $k_F(r) = [3\pi^2\rho(r)/2]^{1/3}$ is the local Fermi momentum.

On the other hand, we have also used the extended Thomas-Fermi (ETF) approximation [22]

$$\tau(\rho) = \alpha\rho(r)^{\frac{5}{3}} + \beta\frac{|(\nabla\rho)|^2}{\rho} + \gamma\nabla^2\rho, \quad (8)$$

where the widely-used values of the parameters α , β , and γ [22]

$$\alpha = \frac{3}{5}(3\pi^2)^{\frac{2}{3}}, \quad \beta = \frac{1}{36}, \quad \gamma = \frac{1}{3} \quad (9)$$

lead to the following expression for the average relative momentum

$$k_{av}^{ETF}(r) = \left[k_F(r)^2 + \frac{5|\nabla\rho(r)|^2}{108\rho^2(r)} + \frac{5\nabla^2\rho(r)}{36\rho(r)} \right]^{\frac{1}{2}}. \quad (10)$$

The MTF kinetic-energy densities for neutrons and protons are shown in Figs. 1(d) and (e), respectively. The kinetic-energy densities derived in the ETF and MTF approximations are in close agreement for ^{93}Nb , as seen in Fig. 1(f). These results prove the consistency of the parametrizations involved. The related $k_{av}(r)$ curves are shown in Figs. 1(g),(h) and (i) for nucleons and ^{93}Nb , respectively. The increased nucleon k_{av} -values at smaller radii follow the behaviour of the $\nabla^2\rho(r)$ for a Fermi distribution, whose importance in the nucleon case results from Eq. (7a).

Furthermore, the local incident momenta $k_i(r)$ calculated for 20 MeV neutrons and protons on ^{93}Nb [7] by using the phenomenological OMP of Lagrange-Lejeune [19] as well as the actual DF potential are also shown in Figs. 1(g) and (h). The minor differences in both shape and magnitude support the use of the Negele-Vautherin approximation [17] as Eq. (4) and the MTF approximation for the calculation of $k_{av}(r)$. The $k_{av}^{MTF}(r)$ curve for the target nucleus ^{93}Nb decreases at larger r , however slower than $k_F(r)$.

The real OMPs for incident neutrons and protons on ^{93}Nb , calculated by means of (i) the single-folding procedure within the LDA, (ii) the complete SF procedure, and (iii) the full DF, are compared with both the phenomenological OMP [19] and the JLM parametrization [3] in Fig. 2. The DDM3Y1-Paris effective NN -interaction, the Fermi density distribution [20] and the MTF approximation for $k_{av}(r)$ have been used in this respect. Moreover, the corresponding volume integrals J_V and *rms* radii $\langle r^2 \rangle^{1/2}$ are given in Table 1. The real part of the JLM potential has been chosen for the present analysis since the parameters of the DDM3Y1 interaction [8,9] was obtained by fitting of the JLM results for the nucleon scattering [3,8,9]. On the other hand, the well-known OMP parameter set of Lagrange-Lejeune [19] has also been computed for both kinds of projectiles on ^{93}Nb , close to the JLM analysis.

First, Fig. 2 shows that more diffuse potentials with larger $\langle r^2 \rangle^{1/2}$ values are obtained for neutrons as well as for protons when the folding procedure increases in accuracy going from NM to DF cases. Actually, the comparison in Figs. 2 (a),(b) and (d),(e) of the real

OMP obtained by using the NM and SF methods evidences the effects of the target nuclear density and the corresponding average relative momentum. Next, the comparison with Figs. 2(c) and (f) shows even stronger effect of the nucleon density distribution and the average relative momentum. On the other hand, the different choices of the target k_{av} (MTF or ETF) have practically no effect on the single-folded real OMP, the corresponding curves in Figs. 2(b) and (e) being overlapped.

Second, the comparison between the real parts of the OMPs shown in Fig. 2 to the phenomenological values [19] and the JLM parametrization [3] is completed by considering the energy dependence of the corresponding volume integrals. From Fig.3 it is seen that the phenomenological and both calculated J_V values from the SF and the DF approach agree rather well. In view of the increasing agreement for the depths (Fig. 2) and the $\langle r^2 \rangle^{1/2}$ values (Table I) in going from the SF to DF procedures these comparisons can be considered an important test of the present calculations. A comment concerning the proton case is necessary. There, the comparison to the JLM parametrization is less significant, because the latter accounts only for the isoscalar component of the full real OMP.

Third, we have considered in the present work three different density-dependent versions DDM3Y1, BDM3Y1 and HLM3Y of the M3Y-Paris and M3Y-Reid NN -interactions. The double-folded real OMPs corresponding to the former interaction for DDM3Y1 and BDM3Y1 are shown in Fig. 4 for the neutron as well as the proton cases. It results that the two density dependences lead to almost identical folded real OMPs provided that a Fermi-distribution of the nucleon density is used. Also, the calculated real part of the OMP using HLM3Y interaction [10] lead to comparable results with those obtained by DDM3Y1 and BDM3Y1. The radial dependence of the real OMP corresponding to the Paris-HLM3Y effective NN -interaction, however evidences enhanced values in the surface region as can be seen from the *rms* radii values in Table 1. On the other hand, an obvious difference exists between the DF real potentials corresponding to the simple M3Y-interaction and the density-dependent versions, respectively.

The density dependence of the effective NN -interaction improves the agreement of the folded potentials with the phenomenological ones by reducing the DF potential values at small values of r where the highest overlap of the interacting projectile and target-nucleus densities takes place. However, the simple M3Y folded potentials are less diffuse in the nuclear surface region, e.g. they have smaller $\langle r^2 \rangle^{1/2}$ values than the real OMPs obtained by means of the energy-dependent NN -interactions (see Table 1).

The importance of the realistic effective NN -interactions is pointed out by showing also in Fig. 4 the DF real potentials calculated by means of the usual 1 fm range Yukawa interaction with the V_0 strength values obtained by Watanabe *et al.* for these systems [23], i.e., $V_0=40$ MeV for $n+^{93}Nb$ and 46.8 MeV for $p+^{93}Nb$. On the other hand, there are also shown the results obtained by using the *equivalent* 1 fm range Yukawa interaction with V_0 strengths corresponding to the volume integral values provided by the Paris-M3Y interaction. Thus, the improvement in comparison with the 1 fm range Yukawa interaction obtained just using the simpler M3Y interaction is obvious. Rather similar effect has the use of the *equivalent* V_0 values, corresponding to the Paris-M3Y volume integrals. Obviously, the supplementary density dependence increases the agreement with the phenomenological optical potentials [see Figs. 2(c)(f)] considerably.

Finally, one comment may concern the effect of the NN -interaction type, i.e. of the Paris

and Reid potentials. As seen from Table 1, the J_V and $\langle r^2 \rangle^{1/2}$ values for the corresponding neutron and proton folded potentials are close to each other, independent of using the NM, SF, and DF. Thus one may conclude that both NN interactions lead to reliable results in folding calculations.

In conclusion, this analysis has shown that the double folding procedure involving the nucleon-density Fermi distribution and average relative momentum leads to real OMPs at lower energies in good agreement with the phenomenological OMPs as well as with the JLM parametrization for both neutron- and proton-nucleus scattering. The analysis of the average effective NN -interaction strength by using the actual folded real OMP and following [7] is in progress. Since this quantity is still considered as the only free parameter of the quantum-statistical studies of the multistep reactions, the corresponding search for the realistic effective NN -interaction at low energies is thus of further interest.

The comparison of the full folding calculations to the results obtained with the strongly simplified single Yukawa description is very instructive showing clearly the restrictions of a "simple" parameterization. Apparently, the depth of the potential is overestimated because of the lack of density dependence, as one should expect. For inelastic transitions at a fixed incident energy one might compensate that shortcoming by simply rescaling the V_0 parameter such that the "local" interaction strength in the reaction region is accounted for in the average. However, the penetration and therefore the interaction region changes with incident energy and Q -value. Very likely, the observed energy dependence of V_0 is actually produced to a large extent by the underlying density dependence which was taken into account explicitly in this work.

A clearer account of that effect could be obtained from elastic and inelastic scattering reaction calculations (OMP and DWBA) at different incident energies where one tries to reproduce the cross sections derived with density dependent interactions by OMPs and form factors from a single Yukawa interaction.

References

- [1] G.R. Satchler, and W.G. Love, Phys. Rep. **55**, 183 (1979); G.R. Satchler *Direct nuclear reactions* (Oxford University Press, Oxford, 1983).
- [2] F.A. Brieva, and J.R. Rook, Nucl. Phys. **A291**, 317 (1977).
- [3] J.-P. Jeukenne, A. Lejeune, and C. Mahaux, Phys. Rev. C **16**, 80 (1977).
- [4] H.F. Arellano, F.A. Brieva, and W.G. Love, Phys. Rev. C **52**, 301 (1995); **50**, 2480 (1994); **43**, 2734 (1991); **41**, 2188 (1990); Phys. Rev. Lett **63**, 605 (1989).
- [5] F.T. Baker, L. Bimbot, C. Djalali, C. Glashauser, H. Lenske, W.G. Love, M. Morlet, E. Tomasi-Gustafson, J. van de Wiele, J. Wambach, A. Willis, Phys. Rep. 289 (1997) 235.
- [6] H. Feshbach, A. Kerman, and S. Koonin, Ann. Phys. (NY) **125**, 429 (1980).
- [7] M. Avrigeanu, A. Harangozo, V. Avrigeanu, and A.N. Antonov, Phys. Rev. **C54**, 2538 (1996); **C56**, 1633 (1997).
- [8] Dao T. Khoa, and W. von Oertzen, Phys. Lett. B **304**, 8 (1993); **342**, 6 (1995); Dao T. Khoa *et al.*, Nucl. Phys. **A602**, 98 (1996).
- [9] Dao T. Khoa, W. von Oertzen, and H.G. Bohlen, Phys. Rev. C **49**, 1652 (1994).
- [10] F. Hofmann, and H. Lenske, Phys. Rev. C **57**, 2281 (1998)
- [11] V. Stoks, R. Timmermans, and J.J. de Swart, Phys. Rev. C **47**, 512 (1993); V.G.J. Stoks, R.A.M. Klomp, M.C.M. Rentmeester, and J.J. de Swart, Phys. Rev. C **48**, 792 (1993); R.B. Wiringa, V.G.J. Stoks, and R. Schiavilla, Phys. Rev. C **51**, 38 (1995).
- [12] V.G.J. Stoks, R.A.M. Klomp, C.P.F. Terheggen, and J.J. de Swart, Phys. Rev. C **49**, 2950 (1994);
- [13] R. Machleidt, Adv. Nucl. Phys. **19**, 189 (1989); R. Machleidt, F. Sammarruca, and Y. Song, Phys. Rev. C **53**, R1483 (1996).
- [14] F. Gross, J.W. van Orden, and K. Holinde, Phys. Rev. C **45**, 2094 (1992)
- [15] F. de Jong, and H. Lenske, Phys. Rev. C **57**, 3099 (1998)
- [16] X. Campi, and A. Bouyssy, Phys. Lett. **73B**, 263 (1978).
- [17] J.W. Negele, and D. Vautherin, Phys. Rev. C **5**, 1472 (1972).
- [18] H. Krivine and J. Treiner, Phys. Lett. **88B**, 212 (1979).
- [19] Ch. Lagrange, and A. Lejeune, Phys. Rev. C **25**, 2278 (1982).
- [20] H. Lenske, (DFS subroutine) (*unpublished*).
- [21] J.W. Negele, Phys. Rev. C **1**, 1260 (1970).
- [22] X. Campi, and S. Stringari, Nucl. Phys. **A337**, 313 (1980).
- [23] Y. Watanabe *et al.*, Phys. Rev. C **51**, 1891 (1995).

Table 1. Volume integrals (in MeV·fm³) and radii $\langle r^2 \rangle^{1/2}$ (in fm) for the real part of folded OMP calculated by means of the nuclear matter (NM), single-folding (SF) and double-folding (DF) procedures, phenomenological OMP [19] and JLM parametrization [3].

Interaction	NM		SF		DF		Phenomenological	
	J_V	$\langle r^2 \rangle^{1/2}$	J_V	$\langle r^2 \rangle^{1/2}$	J_V	$\langle r^2 \rangle^{1/2}$	J_V	$\langle r^2 \rangle^{1/2}$
neutrons								
JLM	404.5	4.652					398.6	4.930
Paris-M3Y	383.0	4.399	402.0	4.692	398.7	5.057		
Paris-HLM3Y	448.3	4.812	470.3	5.072	422.4	5.270		
Paris-HLM3Y*	452.9	4.857						
Paris-BDM3Y1	385.7	4.527	404.9	4.808	384.9	5.168		
Paris-DDM3Y1	395.7	4.567	415.3	4.846	392.2	5.194		
Reid-DDM3Y1	360.2	4.568	383.7	4.854	367.0	5.206		
protons								
							470.1	4.930
Paris-M3Y	429.3	4.413	452.7	4.692	451.4	5.075		
Paris-HLM3Y	501.1	4.793	528.2	5.046	483.0	5.268		
Paris-HLM3Y*	507.7	4.839						
Paris-BDM3Y1	433.1	4.539	456.9	4.808	438.0	5.183		
Paris-DDM3Y1	444.2	4.579	468.6	4.846	446.3	5.209		
Reid -DDM3Y1	422.0	4.584	453.0	4.865	436.4	5.234		

*The Hartree-Fock nuclear density for ⁹³Nb has been used in this case [20].

FIGURE CAPTIONS

FIG. 1. Nuclear density distributions, kinetic-energy densities $\tau(r)$ (MTF, solid curves) and (ETF, dotted curve), the local incident momenta k_i corresponding to the 20 MeV incident energy, and MTF average relative momenta $k_{av}(r)$, for (a,d,g) neutron, (b,e,h) proton, and (c,f,i) the target nucleus ^{93}Nb , respectively. The Fermi-distribution as given by Lenske [20] (solid curves) or Negele parametrization [21] (dotted curves) are used for nucleon density distribution, and only the latter for the target nucleus. The k_i values correspond to the phenomenological OMP of Lagrange-Lejeune (LL) [19] (dashed-dotted curves) and to the DF potential (dashed curves), while the MTF average relative momentum (solid curve), the ETF k_{av} (solid curve), and the local Fermi momentm (dotted curves) are shown for the taget nucleus.

FIG. 2. The radial dependence of the real OMP calculated with the Paris-DDM3Y1 effective NN -interaction in the MTF approximation, by using the nuclear matter approximation (NM), single-folding (SF) and double-folding (DF) procedures (solid curves), compared with the phenomenological OMP [19] (dashed curves) and JLM parametrization [3] (dotted curves), for (a,b,c) neutrons and (d,e,f) protons of 20 MeV incident energy on the target nucleus ^{93}Nb .

FIG. 3. The incident-energy dependence of the volume integrals of real OMP calculated with the Paris-DDM3Y1 effective NN -interaction in the MTF approximation, by using the nuclear matter approximation (NM), single-folding (SF) and double-folding (DF) procedures (solid curves), as well as with the phenomenological OMP [19] (dashed curves) and JLM parametrization [3] (dotted curves), for (a,b,c) neutrons and (d,e,f) protons incident on the target nucleus ^{93}Nb .

FIG. 4. The same as Fig. 2, for (a) neutrons and (b) protons, and corresponding also to the effective NN interactions M3Y (dotted curves), BDM3Y1 (dashed curves), 1 fm range Yukawa with the V_0 values either obtained through FKK analysis [23] (dotted-dashed curves) or equivalent (double dotted-dashed curves) to the M3Y interaction (see text).

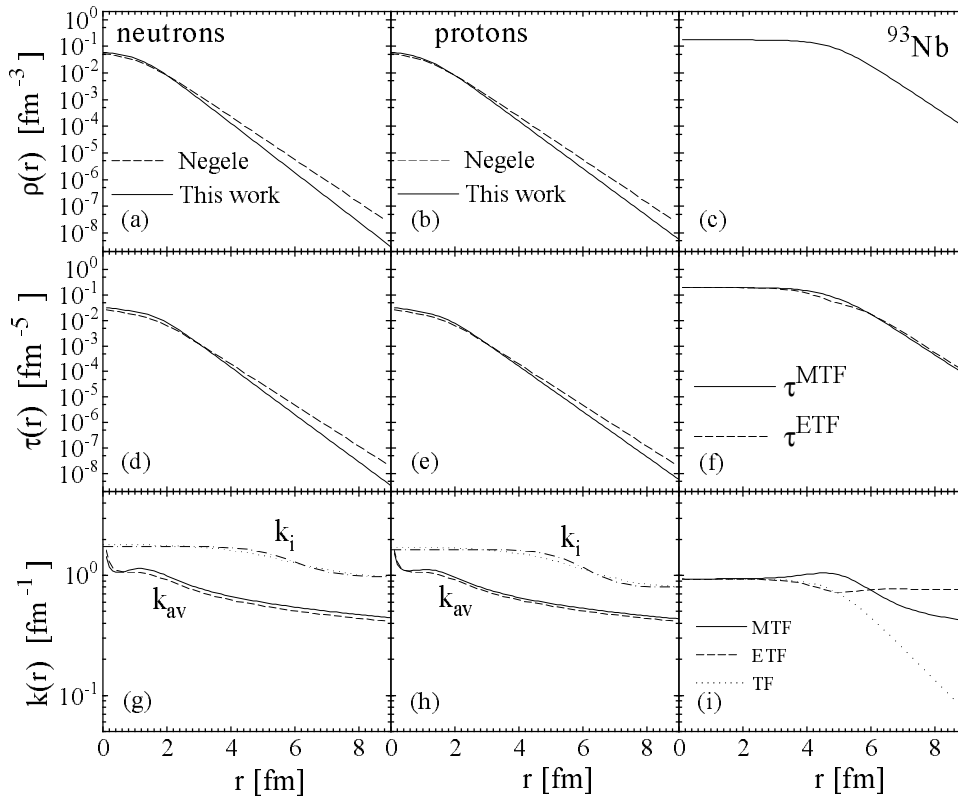


Fig. 1. - M. Avrigeanu

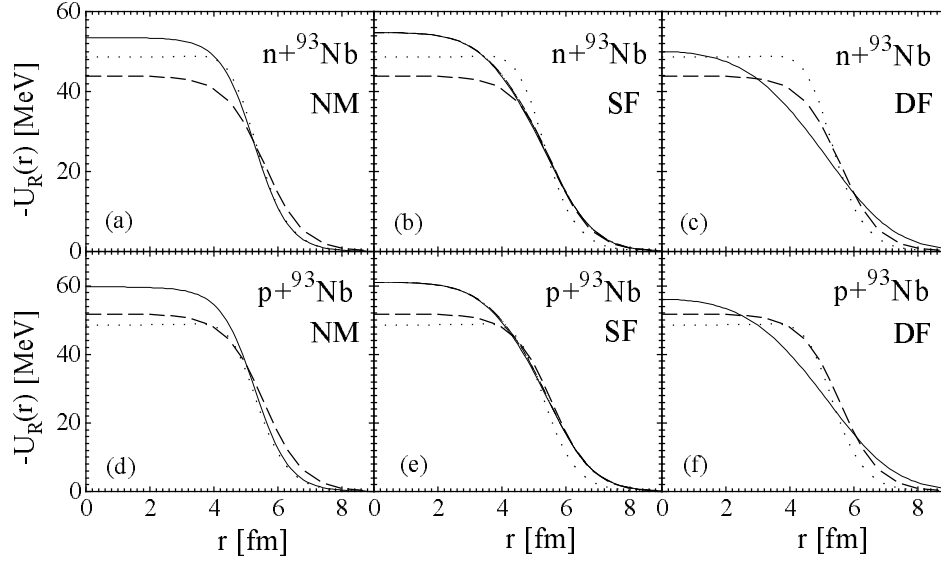


Fig. 2. - M. Avrigeanu

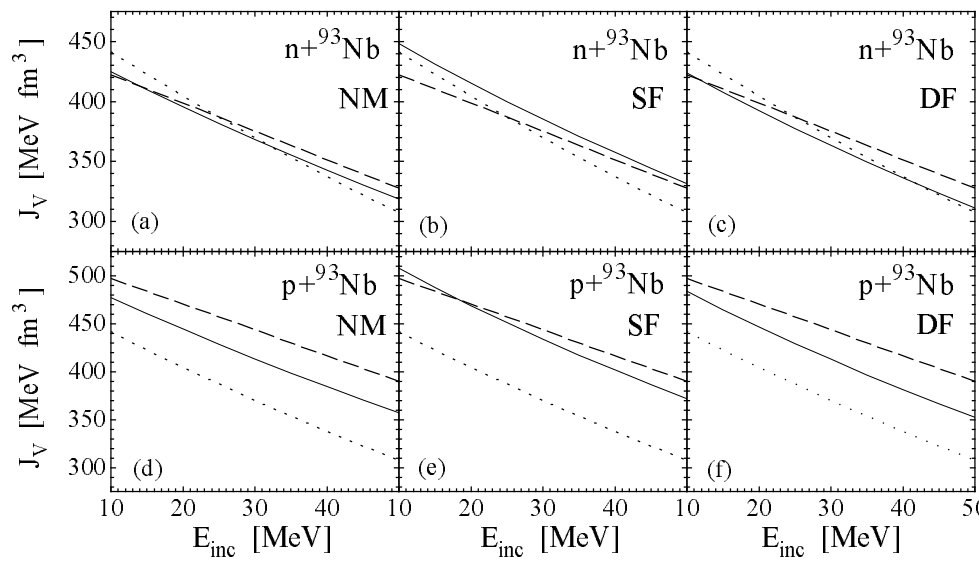


Fig. 3. - M.Avrigeanu

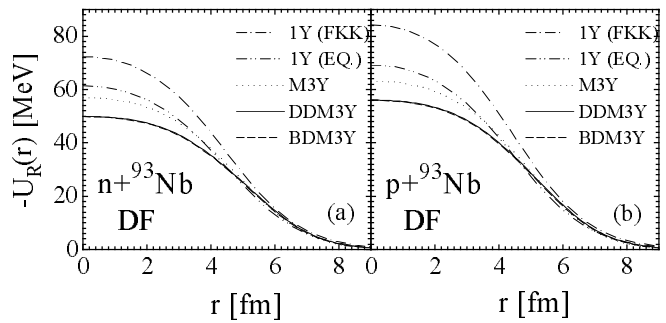


Fig. 4. - M. Avrigeanu